Antiviral Research 91 (2011) 64–71

Contents lists available at ScienceDirect

Antiviral Research

journal homepage: www.elsevier.com/locate/antiviral

Inhibition of rabies virus propagation in mouse neuroblastoma cells by an intrabody against the viral phosphoprotein

Yoshihiro Kaku *, Akira Noguchi, Kozue Hotta, Akio Yamada, Satoshi Inoue

Department of Veterinary Science, National Institute of Infectious Diseases, 1-23-1, Toyama, Shinjuku, Tokyo 162-8640, Japan

ARTICLE INFO

Article history:
Received 2 March 2011
Revised 13 April 2011
Accepted 27 April 2011
Available online 5 May 2011

Keywords:
Rabies
Phosphoprotein
Intrabody
scFv
Intracellular immunization

ABSTRACT

Rabies virus (RABV) is highly neurotropic and causes acute infection of the central nervous system. Death can be averted by prompt post-exposure prophylaxis; however, after clinical symptoms appear, the mortality rate is almost 100% and no reliable treatment is available. In this study, we investigated whether intracellular immunization using single-chain variable fragments (scFvs) against RABV phosphoprotein (RABV-P) could inhibit RABV propagation in neuronal cells. Of four scFv clones derived from an scFv phage-displayed library, scFv-P19 showed extremely high transfection efficiency and stable expression in mouse neuroblastoma (MNA) cells. The intracellular affinity and inhibition of RABV propagation were investigated using RABV-infected MNA cells pretransfected with the scFv-P19 gene. The specific interaction between scFv and RABV-P was confirmed by an immunoprecipitation assay and an indirect immunofluorescence assay showing that these molecules colocalized in the cytoplasm. Measurements of the spread of RABV in a culture well and the virus titer in the supernatant showed that RABV inhibition peaked 3 days after infection, at 98.6% and 99.9% inhibition, respectively. Although the mechanism of RABV inhibition by scFv-P19 is not clear, this scFv-based intracellular immunization could be a candidate for future RABV therapeutic studies if combined with appropriate delivery and application systems.

1. Introduction

Rabies virus (RABV) is a highly neurotropic virus that causes an acute infection of the central nervous system (CNS). RABV inoculated into peripheral tissues is hypothesized to enter nerve terminals either after replication in the peripheral skeletal muscle or directly, without prior replication (reviewed by Schnell et al. (2010)). The virus then travels via retrograde fast axonal transport within axons in peripheral nerves, through the spinal cord and dorsal root ganglia, to brain neurons. Following the invasion of the CNS, the virus rapidly disseminates within the CNS and spreads centrifugally to peripheral sites, including salivary glands, along neuronal routes, which can result in death. Transmission to and excretion from the salivary gland is essential for transmission of RABV to its next host. Death can be averted by prompt post-exposure prophylaxis (PEP). However, if PEP is delayed and clinical symptoms develop, the mortality rate is almost 100%. So far, only a few people have been reported to have survived after the onset of clinical disease (reviewed by Nigg and Walker (2009)). In 2004, it was reported that a patient had survived rabies encephalitis without PEP, after treatment including induction of coma and administration of an antiviral drug (Willoughby et al., 2005). Several laboratories have repeated this treatment program (reviewed by Nigg and Walker (2009)); however, few successful cases have been reported (Hemachudha et al., 2006) and the efficacy of this method is still controversial. To establish more stable and successful therapy, novel neuroprotective approaches based on specific anti-RABV agents are required.

Intracellular immunization (Baltimore, 1988) is a promising therapeutic technique that uses various forms of gene transfer to provide specific cellular resistance to viral infection. One approach is the degradation of viral messenger RNA by gene silencing mediated by antisense oligonucleotides (Stein et al., 2010), ribozymes (Nawtaisong et al., 2009), or RNA interference (RNAi; Dykxhoorn et al., 2003). Another approach is the inhibition of viral protein functions or interactions by intracellularly expressed antibodies, known as intrabodies (Marasco, 1997). Each approach has advantages for therapeutic application (Cao and Heng, 2005). Intrabodies have much higher specificity against target proteins than RNAi and far longer half-lives can be attained; however, intrabodies are more time-consuming and labor-intensive to generate. The most-explored form of intrabody is the single chain variable fragment (scFv), which consists of the VH and VL regions of the variable antigen-binding site of an immunoglobulin, connected with a short linker sequence. The scFvs possess several advantages over immunoglobulins as an intrabody format: a simple and compact structure, higher stability, and increased solubility. Intrabodies

* Corresponding author. Tel.: +81 3 5285 1111; fax: +81 3 5285 1179.
E-mail address: ykaku@nih.go.jp (Y. Kaku).

0166-3542/$ - see front matter © 2011 Elsevier B.V. All rights reserved.
doi:10.1016/j.antiviral.2011.04.016

based on scFvs have been developed against human immunodeficiency virus-1 (Goncalves et al., 2002), hepatitis B virus (Yamamoto et al., 1999), hepatitis C virus (Karthe et al., 2008), rotavirus (Vascotto et al., 2004), herpes virus (Corte-Real et al., 2005), and flavivirus (Jiang et al., 1995). The intrabody-based strategy could be applied to the development of future therapeutic agents against rabies, because RABVs transfer exclusively cell-to-cell and possess highly distinct neurotropism.

In this study, we developed several scFv-based intrabodies against RABV phosphoprotein (RABV-P). RABV-P was chosen as a target for intracellular immunization because it is involved in multiple functions through interactions with various viral or cellular proteins, such as encapsidation of viral genome RNA (Chenik et al., 1994), acting as a cofactor for RABV large protein (RABV-L, a viral RNA polymerase; Chenik et al., 1998), and inhibition of the cellular antiviral system induced by interferons (Vidy et al., 2007). Using a phage-displayed scFv library, we obtained four genetically independent scFv clones. One of these scFvs, when expressed transiently in mouse neuronal cell lines before RABV infection, severely inhibited the propagation and secretion of RABV and the spread of infection. This approach could be a prospective candidate for the establishment of novel therapeutic agents against RABV infection.

2. Materials and methods

2.1. Virus and viral protein

The fixed RABV strain CVS-11 was used in this study. The recombinant RABV-P protein was prepared as described previously (Motoi et al., 2005).

2.2. Selection of scFvs against RABV-P

Human single-fold scFv libraries I + J (Tomlinson I + J; a kind gift from MRC Centre for Protein Engineering, Cambridge, United Kingdom) underwent selection for the ability to bind RABV-P protein. The libraries are based on a single human framework for VH (V3-23/DP-47 and J_H4b) and Vκ (O12/O2/DPK9 and Jκ1) with side chain diversity incorporated at positions in the antigen binding site. In the libraries, the scFv genes were linked to a His-tag followed by a myc-tag and cloned into pIT2 phagemid vectors. The selection or "panning" process was essentially as described by the manufacturer's protocol (http://www.geneservice.co.uk/products/proteomic/datasheets/tomlinsonIJ.pdf). Briefly, Nunc immunotubes (Thermo Fisher, Wiesbaden, Germany) were coated with 100 μg/mL of RABV-P in PBS. After washes with PBS and blocking with PBS containing 2% skim milk, tubes were loaded with 10^{12}–10^{13} phages and incubated for 2 h. After intensive washes, bound phages were eluted by adding 500 μL of trypsin–PBS (2 mg/mL trypsin in PBS). The eluted phages were propagated and amplified in *Escherichia coli* TG1. After three rounds of panning, individual clones were grown in a 96-well U-bottom plate. Phages were produced by adding KM13 helper phages, and the binding to RABV-P by the monoclonal phages was confirmed by enzyme-linked immunosorbent assay (ELISA). As a negative control, scFvs against an unrelated protein, immunoglobulin G (IgG) of the fruit bat *Rousettus aegyptiacus* (a kind gift from Dr. T. Omatsu, Tokyo University) were selected following the same procedure.

2.3. ***ELISA***

The ELISA plate was coated with either native RABV-P (2 μg/well) or denatured RABV-P (2 μg/well); the latter was generated by boiling RABV-P in 2% SDS for 5 min. Nonspecific binding was blocked by PBS containing 5% skim milk. The phages (diluted 1:10) or soluble scFvs (in *E. coli* HB2151 supernatant, diluted 1:10) were added to a set of two wells (native RABV-P and denatured RABV-P antigens) and incubated for 1 h at room temperature. After the plates had been washed, the bound phages were visualized by the addition of horseradish peroxidase (HRP)-conjugated protein L (Pierce, Rockford, IL, USA) and SureBlue TMB 1-component Microwell Peroxidase Substrate (KPL, Gaithersburg, MD, USA). The optical density (OD) was read at 450 nm using a Model 680 Microplate Reader (Bio-Rad, Hercules, CA, USA).

2.4. Phagemid DNA sequencing

The phagemid vector pIT2 was isolated using a Qiagen Plasmid Midi Kit (Qiagen, Venlo, Netherlands). The phagemids were sequenced using the Big Dye Terminator v3.1 Cycle Sequencing Kit (Applied Biosystems, Foster City, CA, USA) with the 373 DNA Sequencer (Applied Biosystems). The primers used to sequence the scFv inserts in the pIT2 vector were LMB3 (5′-CAGGAAACAGCTATGAC-3′) and pHEN (5′-CTATGCGGCCCCATTCA-3′). Deduced amino acid sequences of each α-RABV-P scFv were aligned using GENETYX Ver. 9 (Genetyx, Tokyo, Japan).

2.5. Expression and purification of soluble scFvs

RABV-P-reactive and genetically independent phage clones were selected for induction of soluble scFv production. *E. coli* HB2151 was transformed with phages and inoculated in 2× TY (tryptone–yeast) medium containing 100 μg/mL ampicillin and 0.1% glucose, then grown at 37 °C until the OD_{600} reached approximately 0.5. To induce the expression of soluble scFv, 1 mM isopropyl-β-D-thiogalactapyranoside was added to the culture. After incubation for 4 h at 30 °C, the culture was centrifuged at 2600 *g* for 20 min, and the pellet was resuspended in lysis buffer (50 mM NaH_2PO_4, 300 mM NaCl, and 10 mM imidazole) and incubated on ice for 30 min. After the lysate was divided into aliquots in 2.0-mL tubes, glass beads (Sigma, St. Louis, MO, USA) were added, and the cells were disrupted with a Fast Prep Cell Disrupter (Qbiogene, Carlsbad, CA, USA) at speed 4 for 20 s. Following incubation on ice for 10 min and centrifugation at 12,000*g* for 5 min, the supernatant containing scFv and other *E. coli*-derived proteins was collected. For the purification of scFv, Ni–NTA nickel-charged resin (Qiagen) was added to the supernatant, and the mixture was rotated at 4 °C for 1 h. After centrifugation at 1000 *g* for 10 min, the pelleted Ni–NTA was washed three times with wash buffer (50 mM NaH_2PO_4, 300 mM NaCl, and 20 mM imidazole). Finally, scFv was eluted using elution buffer (50 mM NaH_2PO_4, 300 mM NaCl, and 250 mM imidazole).

2.6. Immunoprecipitation

To examine the interaction between scFv and RABV-P *in vitro*, immunoprecipitation of *E. coli*-expressed soluble scFv against RABV-P was performed using magnetic beads (Dynabeads His-Tag Isolation & Pulldown; Invitrogen, Carlsbad, CA, USA). Briefly, mouse neuroblastoma (MNA) cells were grown as a monolayer in 6-well plates, infected with RABV at a multiplicity of infection (m.o.i.) of 10, and subsequently incubated in a 5% CO_2 incubator. After 48 h, the cells were lysed with 0.5 mL of lysis buffer (50 mM sodium phosphate [pH 8.0], 300 mM NaCl, 0.01% [vol/vol] Tween-20, 1% [vol/vol] Triton-X 100) at 4 °C for 1 h. The cell lysates were centrifuged at 20,000*g* for 30 min at 4 °C. The supernatants were collected, and 2.5 μg of scFvs were added and reacted for 1 h at 4 °C. The samples were mixed with Dynabeads and incubated for 10 min, washed four times with wash buffer (50 mM sodium phosphate [pH 8.0], 300 mM NaCl, 0.01% [vol/vol] Tween-20), and then

resuspended in 20 μL loading buffer (containing 4× NuPAGE LDS Sample Buffer [Invitrogen, Carlsbad, CA, USA], 10× NuPAGE Reducing Agent [Invitrogen]). After heating the sample for 10 min at 70 °C, the samples were subjected to SDS–polyacrylamide gel electrophoresis (PAGE).

To confirm the *in vivo* interaction between the intrabody and RABV-P, immunoprecipitation was performed using a Dynabeads Protein G Immunoprecipitation Kit (Invitrogen) and lysates of scFv-transfected MNA cells with or without RABV infection. To make the cell lysates, scFv-P19-pCAG was first transfected into MNA cells as described below (see Section 2.10). After 24 h, the cells were infected with CVS-11 (m.o.i. = 10) or mock-infected. At 48 h after infection, the cells were lysed, centrifuged, and collected as described above. The manufacturer's immunoprecipitation protocol was followed, using the buffer set included in the Kit. Briefly, 1.5 mg of Dynabeads were mixed with 2.0 μg of an anti-myc tag mouse monoclonal antibody (MoAb; MBL, Nagoya, Japan) and reacted for 10 min at room temperature. After washes with Ab Binding & Washing Buffer, the cell lysates were added and reacted for 10 min. After washes with Washing Buffer, the samples were suspended in a mixture of 20 μL Elution Buffer and 10 μL loading buffer. The samples were eluted by heating for 10 min at 70 °C, and were subjected to SDS–PAGE.

2.7. SDS–PAGE and Western blotting

The precipitated proteins were suspended in loading buffer and separated by electrophoresis in NuPAGE Novex Bis–Tris Mini Gels (Invitrogen) using MES Buffer (Invitrogen). In the upper buffer chamber, NuPAGE Antioxidant (Invitrogen) was added at a concentration of 0.25%. After SDS–PAGE, the proteins were transferred onto PVDF membranes using a semidry transblotter (Bio-Rad). The membranes were blocked for 1 h at room temperature (or overnight at 4 °C) with 5% skim milk (wt/vol) in PBS.

To detect RABV-P, a rabbit anti-RABV-P polyclonal antibody, obtained by DNA immunization, was diluted 1:5000 with 1% skim milk in PBS containing 0.05% (vol/vol) Tween-20 (PBS-T) and incubated with the membranes for 1 h at room temperature. Following four washes with PBS-T, an HRP-conjugated anti-rabbit IgG, diluted 1:5000 with 1% skim milk in PBS-T, was added and incubated for 1 h at room temperature. After four washes, the membranes were developed with ECL Plus Western Blotting Detection Reagent substrate solution (GE Healthcare). The signals were detected using VersaDoc (Bio-Rad).

To detect scFvs, an anti-myc tag mouse MoAb; was added to the primary antibody solution (above) at 0.5 μg/100 μL, and HRP-conjugated goat anti-mouse IgG (H + L) (Pierce) was added to the secondary antibody solution (above) at 1:5000.

2.8. Characterization of scFv affinity

To characterize the affinity of each scFv, ELISA against immobilized RABV-P was performed using peroxidase-labeled scFvs. First, 200 μg of each soluble scFv was peroxidase-labeled using a Peroxidase Labeling Kit-NH_2 (Dojindo, Kumamoto, Japan) in accordance with the manufacturer's instructions. After the labeling, serially diluted scFvs were applied to an ELISA plate coated with native RABV-P and detected as described above (see Section 2.3). The OD data was graphed by using Prism 5 (GraphPad, San Diego, CA, USA).

2.9. scFv vectors for intrabody expression

Each scFv gene cDNA was recovered from its pIT2 phagemid vector by PCR (primer sequences will be supplied on request). For intrabody expression, each scFv gene cDNA was inserted into pCAGGS-derived pCAGJ12bsr (Kojima et al., 2003; a kind gift from Dr. Asato Kojima, National Institute of Infectious Diseases, Japan), after the removal of the original insert, J12. The generated vectors were named scFv-P19-pCAG, scFv-P38-pCAG, scFv-P80-pCAG, scFv-P115-pCAG, and scFv-bat-IgG-pCAG (negative control).

2.10. Transfection and confirmation of intrabody expression

Each intrabody expression vector was transfected into MNA cells using Fugene HD (Roche) in accordance with the manufacturer's protocol. At 1–4 days after transfection, intrabody expression was confirmed with an indirect immunofluorescence assay (IFA). Briefly, after cell fixation in 3.6% formaldehyde and 0.4% Triton-X for 30 min at room temperature, the intrabody was stained using the anti-myc tag mouse MoAb as the primary antibody and an FITC-goat anti-mouse IgG (H + L) (Invitrogen) as the secondary antibody, then viewed under a fluorescence microscope (Nikon, Tokyo, Japan). For counterstaining, 0.002% Evans blue was added to the secondary antibody fluid.

2.11. Confirmation of the interaction between the intrabody and RABV-P in vivo

scFv-P19-pCAG was transfected into MNA cells as described above. After 24 h, the cells were infected with CVS-11 (m.o.i. = 10). At 24 h after infection, the cells were fixed in 3.6% formaldehyde and 0.4% Triton-X. The intrabody was stained as described above, and RABV-P was stained with rabbit anti-RABV-P serum as the primary antibody and TRITC-conjugated anti-rabbit IgG (Sigma) as the secondary antibody. Cells were visualized and the images were digitally captured by a BZ-8000 "Bio-zero" fluorescence microscope (KEYENCE, Osaka, Japan). At 24 h after transfection, the cells were lysed and collected, and then immunoprecipitated as described above.

2.12. Measurement of inhibition of RABV propagation by the intrabody

scFv-P19-pCAG was transfected into MNA cells in a 96-well plate as above. After 24 h, the cells were infected with CVS-11 (m.o.i. = 0.005). At 1 to 4 days after infection, inhibition of RABV propagation by the intrabody was measured by two methods: (i) measurement of the proportion of an area infected with RABV, and (ii) virus titration of the supernatant. To measure the infected area, the cells were stained with FITC Anti-Rabies Monoclonal Globulin (Fujirebio Diagnostics, Malvern, PA, USA), which targets RABV nucleoprotein (RABV-N). Images of RABV-infected (RABV-N-positive) cells were captured digitally as described above. In the digital image, the proportion of the fluorescence-emitting area relative to the whole well was calculated by using VH-H1A5 "VH analyzer" software (KEYENCE), then the data were graphed by using Prism 5. To measure the viral titer, the supernatant was collected, diluted 10-fold serially, and inoculated into MNA cells. After 48 h, the cells were stained by FITC Anti-Rabies Monoclonal Globulin and titrated by the Reed & Muench method (Reed and Muench, 1938).

3. Results

3.1. Selection of scFv clones against RABV-P

After three rounds of panning, a total of 192 phage clones were obtained. The binding ability of these phage clones was examined by ELISA against native RABV-P and denatured RABV-P, and 10 clones that showed equivalent reactivity for both native and denatured RABV-P were selected. DNA sequencing of scFv cDNA in each

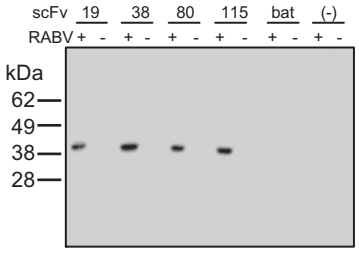

Fig. 1. *In vitro* interaction between scFvs and RABV-P confirmed by immunoprecipitation and Western blotting assays. Western blot analysis of lysates of RABV-infected and mock-infected MNA cells. The lysates were mixed with each scFv (scFv-P19, -38, -80, -115, -bat-IgG) or no scFv and immunoprecipitated with Dynabeads, blotted, and detected with a rabbit anti-RABV-P polyclonal antibody and HRP-conjugated anti-rabbit IgG.

of the 10 clones indicated that these clones converged to four genetically independent clones (Supplemental Fig. 1). *E. coli* HB2151 cells were infected with these phages to obtain soluble scFv for further characterization. After the purification of soluble scFvs using Ni–NTA resin, SDS–PAGE was performed to confirm the expression of scFvs. All four scFv clones showed a single protein band with a molecular weight of 29 kDa by SDS–PAGE (Supplemental Fig. 2). These scFvs were also confirmed to detect RABV-P by reducing Western blot analysis (data not shown), indicating that all four scFvs recognize linear epitopes.

We further performed an immunoprecipitation assay to examine the interaction *in vitro* between these scFvs and RABV-P. RABV-infected MNA cells were lysed 48 h after infection and incubated with each scFv. The protein mixture was precipitated by using magnetic beads to bind the histidine-tagged proteins. A distinct interaction between the scFvs and RABV-P was detected in a Western blot analysis with anti-RABV-P serum (Fig. 1) and the anti-myc MoAb (data not shown). To characterize the affinity of each scFv, we performed ELISA against immobilized RABV-P using peroxidase-labeled scFvs. According to the reaction curves (Supplemental Fig. 3), the affinity against RABV-P was highest in scFv-P19, followed by -115, -38, and -80.

3.2. Confirmation of intrabody expression

The scFv cDNAs of all four clones were inserted into pCAGGS-derived vectors to achieve intracellular expression as intrabodies. The generated intrabody expression vectors, scFv-P19-pCAG, scFv-P38-pCAG, scFv-P80-pCAG, and scFv-P115-pCAG, were transfected into MNA cells for transient expression, and their expression levels were monitored by IFA using an anti-myc tag MoAb. The transfection efficiency of the clones varied: scFv-P19 showed much higher transfection efficiency than the others, reaching more than 80% (estimated by eye; Fig. 2, top). Interestingly, all the scFv clones, but especially scFv-P19, showed highly stable expression without substantial diminution from 24 h until 96 h after transfection (Fig. 2). Considering its high transfection efficiency and stable expression, we selected scFv-P19 for further studies to examine *in vivo* binding with RABV-P and the ability to abrogate viral propagation.

3.3. Confirmation of the interaction between intrabodies and RABV-P *in vivo*

To examine the interaction between the scFv-P19 intrabody and RABV-P *in vivo*, MNA cells were transfected with scFv-P19-pCAG for transient expression, and 24 h later, the same cells were infected with CVS-11 (m.o.i. = 10). At 48 h after infection, intracellular localization of scFvs and RABV-P was observed by IFA using the anti-myc tag MoAb and anti-RABV-P polyclonal serum and compared with the localization in mock-infected MNA cells expressing scFv-P19. In mock-infected MNA cells, scFvs were located diffusely throughout the cytoplasm (Fig. 3A) without any particular condensation of fluorescence. In contrast, in CVS-11-infected MNA cells, some cells showed punctate fluorescent patterns against the background of diffuse fluorescence in the cytoplasm (Fig. 3B). We also observed this punctate fluorescence in CVS-11-infected cells stained with anti-RABV-P polyclonal serum (Fig. 3C), which is typically seen in cells infected with fixed RABV strains in culture and reportedly involves the intracellular accumulation of ribonucleoprotein complex to form Negri bodies (Lahaye et al., 2009). These punctate fluorescent patterns of scFv-P19 and RABV-P overlapped

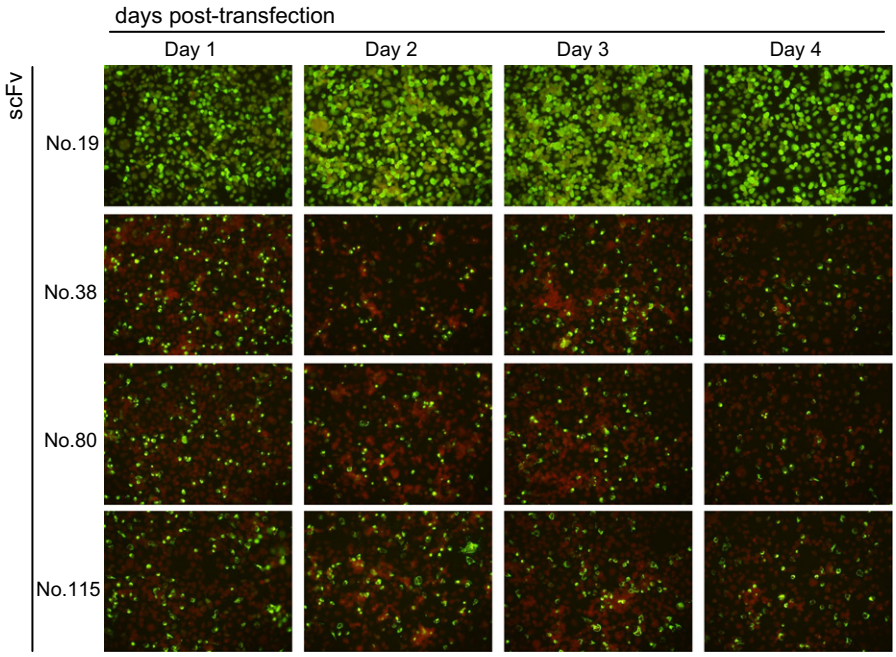

Fig. 2. Time course of intracellular expression of scFvs. In MNA cells transfected with the indicated scFv vectors, scFv was detected by a mouse anti-myc tag MoAb and FITC-conjugated anti-mouse IgG on days 1–4 after transfection. For counterstaining, 0.002% Evans blue was added to the secondary antibody fluid.

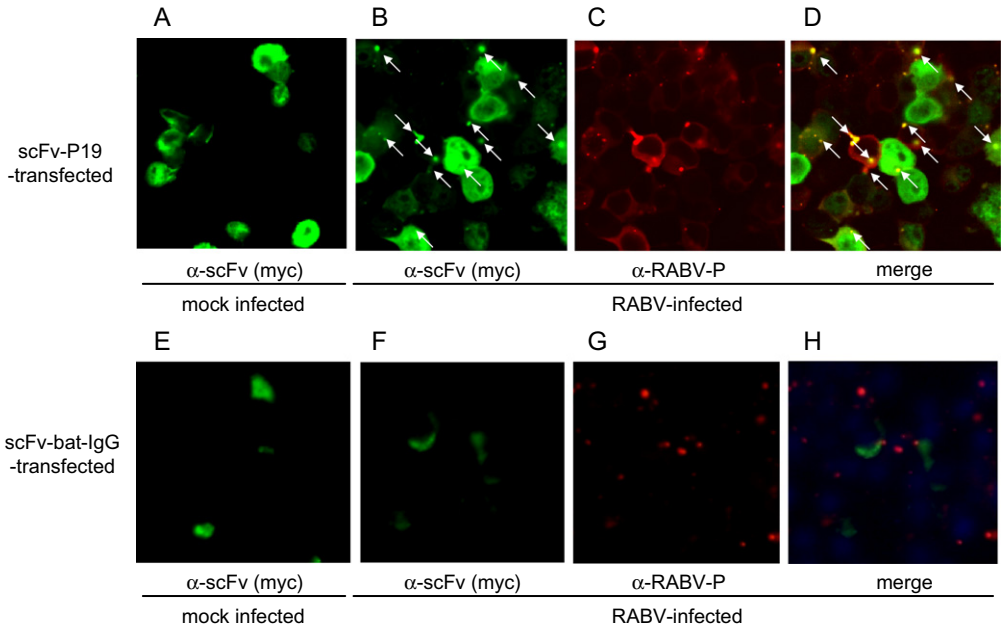

Fig. 3. Intracellular colocalization of scFv-P19 and RABV-P. MNA cells were pre-transfected with scFv-P19-pCAG (A–D) or scFv-bat-IgG-pCAG (E–H). In mock-infected MNA cells pre-transfected with scFv-expressing plasmids (A and E), scFv was detected with an anti-myc tag MoAb and FITC-conjugated anti-mouse IgG. In RABV-infected MNA cells pre-transfected with scFv-expressing plasmids, scFv was detected as described above (B and F) and RABV-P was detected with a rabbit anti-RABV-P polyclonal antibody and TRITC-conjugated anti-rabbit IgG (C and G). (D and H) Merged images of (B) and (C), or (F) and (G). Arrows in (B) and (D) indicate the punctate fluorescence of scFvs.

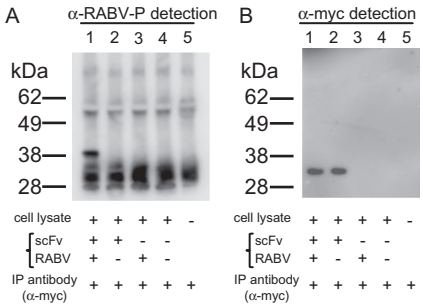

Fig. 4. *In vivo* interaction between scFv-P19 and RABV-P confirmed by immunoprecipitation and Western blotting assays. Western blot analysis of lysates of RABV-infected and mock-infected MNA cells transiently expressing scFv-P19. For detecting RABV-P (A), the lysates were immunoprecipitated (IP) with an anti-myc-tag MoAb, and the immunoblot was probed with a rabbit anti-RABV-P polyclonal antibody and detected by HRP-conjugated anti-rabbit IgG. For detecting scFv-P19 (B), the lysates were IP as above, and the immunoblot was probed with a mouse anti-myc tag MoAb and detected by HRP-conjugated anti-mouse IgG. In both images, cell lysates were immunoprecipitated (+, lanes 1–4) or only lysis buffer was used (–, lane 5). To prepare cell lysates, scFv-P19 was pre-transfected (+, lanes 1 and 2) or not transfected (–, lanes 3 and 4). After 24 h, the cells were inoculated with RABV (+, lanes 1 and 3) or mock-infected (–, lanes 2 and 4). In (A), the bands smaller than 30 kDa appear to be non-specific, because lane 5 (containing only the IP antibody) also has these bands. These non-specific bands might be due to the cross-reactivity of the detection antibody (anti-RABV-P) or the secondary antibody (anti-rabbit IgG) with the IP antibody.

in a merged image (Fig. 3D), indicating that these two molecules colocalized in the cytoplasm. In contrast, in MNA cells pre-transfected with scFv-bat-IgG-pCAG, the change in the fluorescence pattern of scFv was not observed after RABV infection even though the transfection efficiency was much lower than that of scFv-P19-pCAG, and the fluorescence of scFv and RABV-P did not overlap (Fig. 3E–H).

Subsequently, to obtain direct evidence of intracellular binding between scFv-P19 and RABV-P, we immunoprecipitated a lysate of CVS-11-infected MNA cells expressing scFv-P19 with an anti-myc MoAb 48 h after infection. A Western blot analysis using anti-RABV-P polyclonal serum (Fig. 4A) and the anti-myc MoAb (Fig. 4B) showed a 38-kDa RABV-P band (Fig. 4A, lane 1) and a 29-kDa scFv band (Fig. 4B, lane 1), whereas only the scFv band was present in mock-infected cells (Fig. 4B, lane 2). This indicates that these two molecules, scFv-P19 and RABV-P, can associate with each other when co-expressed in the cytoplasm.

Taken together, these results suggest that scFv-P19 is able to recognize and bind to the target protein, RABV-P, intracellularly and to function as an intrabody.

3.4. Inhibition of RABV propagation by the intrabody

Finally, we determined the inhibitory effect of intracellularly expressed scFv-P19 on RABV propagation. MNA cells in 96-well plates were transiently transfected with scFv-P19-pCAG, and 24 h later the cells were infected with CVS-11 at an m.o.i. of 0.005. In this assay, we aimed to observe how the intrabody could inhibit the spread of RABV infection from a limited initial area to simulate the early phase of real viral infection *in vivo*. In order to have the infected area as limited as possible on day 1, we used a low m.o.i. here. We used two separate methods to compare the inhibitory effect of scFv-P19 in scFv-expressing cells and nontransfected cells: measuring the inhibition of the spread of RABV-infected cells in a culture plate (Figs. 5 and 6A), and titration of viruses in the supernatant (Fig. 6B). The data were collected for 4 days after the infection, during which the intracellular expression of scFv-P19 was high and stable (Fig. 5, bottom panel). Cells expressing scFv-P19 substantially inhibited the spread of the RABV-infected area for 4 days (Fig. 5, middle panel), whereas in nontransfected control cells, RABV infection had spread throughout the well within that time (Fig. 5, top panel). The highest inhibitory effect (calculated from the ratio of the proportion of RABV-infected cells in scFv-expressing cells to that in nontransfected cells) was achieved at 3 days after infection ($[1-0.91/66.99] \times 100 = 98.6\%$ inhibition; Fig. 6A). In the experiment involving virus titration, the highest inhibitory effect (calculated from the ratio of the virus titer in

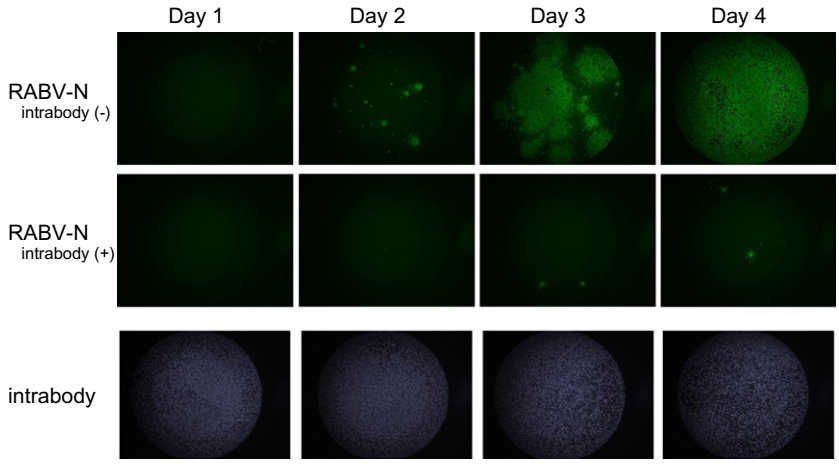

Fig. 5. Comparison of the spread of RABV infection between intrabody-positive and intrabody-negative MNA cells. CVS-11-infected MNA cells without pre-expression of scFv-P19 (top panel), or with pre-expression (middle and bottom panel). The infected cells were stained by FITC Anti-Rabies Monoclonal Globulin on days 1–4 after infection, and the areas that stained positive were compared. In the bottom panels, scFv expression was monitored by staining with a mouse anti-myc tag MoAb and FITC-conjugated anti-mouse IgG; FITC-derived images of scFvs were digitally converted to violet color to avoid confusion with the FITC-derived images of RABV-N in the top and middle panels.

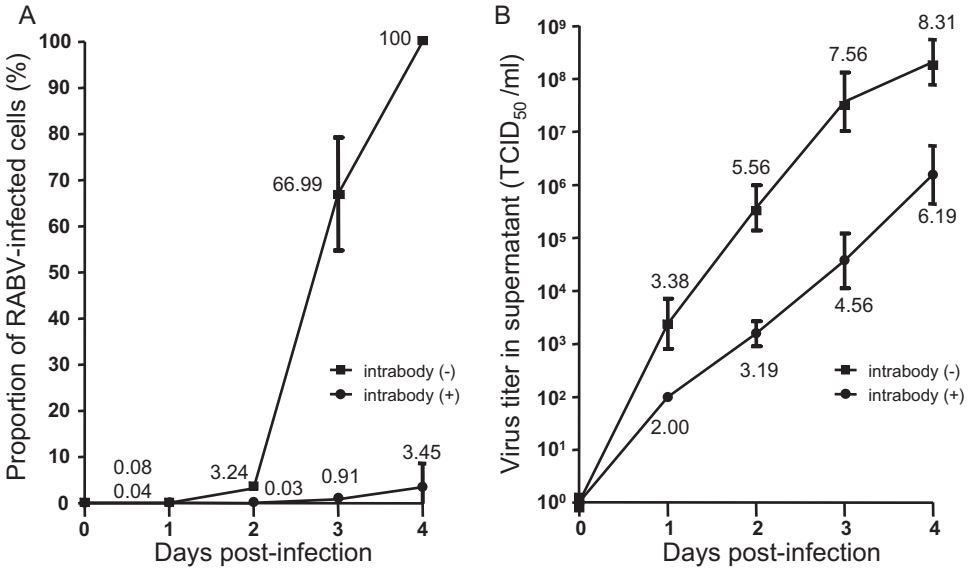

Fig. 6. Inhibition of RABV propagation in MNA cells by intrabody scFv-P19. (A) Time course of the proportion of RABV-infected area relative to the whole well, in a 96-well plate of CVS-11-infected MNA cells without pre-expression of scFv-P19 (■), or with pre-expression of scFv-P19 (●); data were derived from the digitally captured images shown in Fig. 5. Values are mean ± standard error of the mean (SE); $N = 4$. (B) Time course of the virus titer ($TCID_{50}$/ml) in the supernatant of CVS-11-infected MNA cells without pre-expression of scFv-P19 (■), or with pre-expression of scFv-P19 (●). Values are mean ± SE; $N = 4$. The numbers on the graph indicate the logarithm of the mean.

scFv-expressing cells to that in nontransfected cells) was also achieved at 3 days after infection ($[1-10^{4.56}/10^{7.56}] \times 100 = 99.9\%$ inhibition; Fig. 6B)

These results indicate that scFv-P19, when expressed intracellularly as an intrabody, is effective at inhibiting RABV propagation until at least 4 days after infection.

4. Discussion

To our knowledge, this is the first report of intrabody-mediated inhibition of RABV propagation and secretion in studies using mouse neuronal cell lines. A significant reduction in RABV propagation was achieved by pretransfection of an scFv expression vector expressing scFv-P19, which was directed against RABV-P. Another intracellular immunization approach against RABV infection, RNAi-based gene silencing, has also been reported to inhibit RABV propagation (Brandao et al., 2007) and to reduce the replication of the viral genome in mouse neuronal cell lines (Israsena et al., 2009). Also, the intracellular expression of peptides mimicking the N-terminus of RABV-P has been shown to have antiviral activity (Castel et al., 2009). However, no studies of antibody-based intracellular immunization aimed at future therapeutic application have been reported, although several research groups have been developing scFvs or Fabs against RABV proteins for diagnosis or prevention. Intracellular immunization based on scFvs is worthy of investigation because scFvs have several advantages, such as high specificity and long half-lives. Many studies have utilized hybridomas producing MoAbs as a source of scFv; however, phage-display libraries have also been used in recent studies be-

cause they provide benefits such as high diversity in the antigenic repertoire and the ability to rapidly select specific antibodies without animal immunization. In this study, we used human single-fold scFv libraries, Tomlinson I + J, to select scFvs against RABV-P.

One of the obstacles to using scFvs or other antigen-binding molecules as intrabodies is the need to preserve their affinity *in vivo*. Many scFvs have been reported to fold incorrectly *in vivo* and to lose their affinity due to the highly reducing conditions inside cells (Ramm et al., 1999; Wörn and Plückthun, 2001). To minimize this problem, our screening procedure was designed to focus on the selection of scFvs recognizing linear epitopes. Both native and denatured antigens were used as coating antigens in ELISA screening, and only clones showing equivalent reactivity against both were selected. Consequently, all four scFvs obtained in this study reacted with RABV-P in a reducing Western blot analysis, indicating that these clones recognize linear epitopes as expected. Considering the substantial inhibition that scFv-P19 showed against RABV propagation, the strategy of targeting scFv recognizing linear epitopes might be generally useful for future intrabody studies.

We chose RABV-P as the target protein because it contributes to diverse functions through interactions with several viral and cellular proteins. These functions occur at various stages of the RABV life cycle and include encapsidation of viral genome RNA (together with RABV-N and -L), acting as a cofactor for viral RNA polymerase (RABV-L), and inhibiting the interferon-induced cellular antiviral system by binding to signal transducer and activator of transcription 1 (STAT1) and STAT2 to retain them in the cytoplasm (reviewed by Schnell et al., 2010). These multiple functions of RABV-P may be achieved by its efficient modular organization (Gerard et al., 2009) and by the synthesis of four N-terminally truncated P products (P2–P5) showing different subcellular localizations (Blondel et al., 2002): full-length P and P2 are located in the cytoplasm, whereas P3, P4, and P5 are in the nucleus. The detailed three-dimensional structure of P has only been obtained for its C-terminal domain, and how it produces these multiple functions through interactions with various protein counterparts is still not fully understood. The intrabodies against RABV-P obtained in this study were expected to inhibit at least one of these functions, leading to the eradication of viral propagation. Because the epitopes recognized by scFv-P19 (and other clones) have not yet been determined, at the moment there is no evidence regarding which RABV-P function(s) these scFvs block. Our observation that scFv-P19 colocalized with RABV-P in Negri bodies, as well as being diffusely distributed in the cytoplasm, raises the possibility that scFv-P19 inhibits several RABV-P functions in different subcellular locations. Negri bodies, composed of RABV ribonucleoproteins (RABV-N, -P, -L proteins and the RABV genome) and several cellular proteins, are considered to be a marker of RABV infection and are key structures for the synthesis of descendant viral particles (Lahaye et al., 2009). To understand the mechanism through which the scFvs inhibit viral propagation, epitope mapping of the scFvs combined with detailed three-dimensional analysis of RABV-P will be required.

In this study, pretransfection of the scFv-P19 gene into MNA cells substantially inhibited the propagation of RABVs and reduced the virus titer in the supernatant to 1:1000 of that of nontransfected cells at 3 days after infection. This indicates that scFv-P19 could be a prospective candidate for an intrabody; however, this remarkable inhibition might have been achieved partially due to an unexpectedly higher transfection efficiency compared to other scFv clones (scFv-P38, -80, and -115). Although the cause of the difference in transfection efficiency is not clear, a more stable and reliable expression and delivery system should be explored in future studies. One plausible option would be to use a viral vector, which would enable both higher transfection efficiency and strict tropism. These features are especially advantageous for therapeutic application against RABV, which shows extremely high tropism for neuronal cells and propagates by cell-to-cell transmission. By using a viral vector, the other three clones we identified (scFv-P38, -80, and -115), which were not explored further in this study due to low transfection efficiency, might attain higher expression and an inhibition potency as powerful as scFv-P19.

Intrabody research generally consists of two dimensions: the determination of a candidate molecule as an intrabody, and the establishment of an appropriate delivery or application system. This study is the first to report the identification of a candidate molecule that reduces RABV propagation when pretransfected. However, considering the potential of intrabodies as therapeutic tools against RABV infection, post-exposure applications should also be investigated. In this study, we were not able to examine post-exposure application of intrabodies because the high transfection efficiency required for a post-exposure study could not be attained with the transient expression system used. A combination of the scFvs generated in this study and efficient delivery systems involving viral vectors could be powerful tools for future practical studies of post-exposure applications.

In conclusion, we demonstrated that scFv-P19, when pre-expressed as an intrabody in MNA cells, substantially inhibited the propagation of RABV CVS-11. This scFv-based intracellular immunization could be a candidate for a future therapeutic tool against RABV infection if combined with an appropriate delivery and application system, such as a viral vector.

Acknowledgment

This study was supported in part by Health and Labor Sciences Research Grants from Research on International Cooperation in Medical Science. We are grateful to Dr. Mitsuru Sato of the National Institute of Agrobiological Sciences for providing expertise on generating intrabodies.

Appendix A. Supplementary data

Supplementary data associated with this article can be found, in the online version, at doi:10.1016/j.antiviral.2011.04.016.

References

Baltimore, D., 1988. Gene therapy. Intracellular immunization. Nature 335, 395–396.

Blondel, D., Regad, T., Poisson, N., Pavie, B., Harper, F., Pandolfi, P.P., De Thé, H., Chelbi-Alix, M.K., 2002. Rabies virus P and small P products interact directly with PML and reorganize PML nuclear bodies. Oncogene 21, 7957–7970.

Brandao, P.E., Castilho, J.G., Fahl, W., Carnieli, P., Oliveira Rde, N., Macedo, C.I., Carrieri, M.L., Kotait, I., 2007. Short-interfering RNAs as antivirals against rabies. Braz. J. Infect. Dis. 11, 224–225.

Cao, T., Heng, B.C., 2005. Intracellular antibodies (intrabodies) versus RNA interference for therapeutic applications. Ann. Clin. Lab. Sci. 35, 227–229.

Castel, G., Chtéoui, M., Caignard, G., Préhaud, C., Méhouas, S., Réal, E., Jallet, C., Jacob, Y., Ruigrok, R.W.H., Tordo, N., 2009. Peptides that mimic the amino-terminal end of the rabies virus phosphoprotein have antiviral activity. J. Virol. 83, 10808–10820.

Chenik, M., Chebli, K., Gaudin, Y., Blondel, D., 1994. In vivo interaction of rabies virus phosphoprotein (P) and nucleoprotein (N): existence of two N-binding sites on P protein. J. Gen. Virol. 75, 2889–2896.

Chenik, M., Schnell, M., Conzelmann, K.K., Blondel, D., 1998. Mapping the interacting domains between the rabies virus polymerase and phosphoprotein. J. Virol. 72, 1925–1930.

Corte-Real, S., Collins, C., Aires da Silva, F., Simas, J.P., Barbas, C.F., Chang, Y., Moore, P., Goncalves, J., 2005. Intrabodies targeting the Kaposi sarcoma-associated herpesvirus latency antigen inhibit viral persistence in lymphoma cells. Blood 106, 3797–3802.

Dykxhoorn, D.M., Novina, C.D., Sharp, P.A., 2003. Killing the messenger: short RNAs that silence gene expression. Nat. Rev. Mol. Cell Biol. 4, 457–467.

Gerard, F.C.A., Ribeiro, E.D.A., Leyrat, C., Ivanov, I., Blondel, D., Longhi, S., Ruigrok, R.W.H., Jamin, M., 2009. Modular organization of rabies virus phosphoprotein. J. Mol. Biol. 388, 978–996.

Goncalves, J., Silva, F., Freitas-Vieira, A., Santa-Marta, M., Malhó, R., Yang, X., Gabuzda, D., Barbas, C., 2002. Functional neutralization of HIV-1 Vif protein by intracellular immunization inhibits reverse transcription and viral replication. J. Biol. Chem. 277, 32036–32045.

Hemachudha, T., Sunsaneewitayakul, B., Desudchit, T., Suankratay, C., Sittipunt, C., Wacharapluesadee, S., Khawplod, P., Wilde, H., Jackson, A.C., 2006. Failure of therapeutic coma and ketamine for therapy of human rabies. J. Neurovirol. 12, 407–409.

Israsena, N., Supavonwong, P., Ratanasetyuth, N., Khawplod, P., Hemachudha, T., 2009. Inhibition of rabies virus replication by multiple artificial microRNAs. Antiviral Res. 84, 76–83.

Jiang, W., Venugopal, K., Gould, E.A., 1995. Intracellular interference of tick-borne flavivirus infection by using a single-chain antibody fragment delivered by recombinant Sindbis virus. J. Virol. 69, 1044–1049.

Karthe, J., Tessmann, K., Li, J., Machida, R., Daleman, M., Häussinger, D., Heintges, T., 2008. Specific targeting of hepatitis C virus core protein by an intracellular single-chain antibody of human origin. Hepatology 48, 702–712.

Kojima, A., Yasuda, A., Asanuma, H., Ishikawa, T., Takamizawa, A., Yasui, K., Kurata, T., 2003. Stable high-producer cell clone expressing virus-like particles of the Japanese encephalitis virus e protein for a second-generation subunit vaccine. J. Virol. 77, 8745–8755.

Lahaye, X., Vidy, A., Pomier, C., Obiang, L., Harper, F., Gaudin, Y., Blondel, D., 2009. Functional characterization of Negri bodies (NBs) in rabies virus-infected cells: evidence that NBs are sites of viral transcription and replication. J. Virol. 83, 7948–7958.

Marasco, W.A., 1997. Intrabodies: turning the humoral immune system outside in for intracellular immunization. Gene Ther. 4, 11–15.

Motoi, Y., Inoue, S., Hatta, H., Sato, K., Morimoto, K., Yamada, A., 2005. Detection of rabies-specific antigens by egg yolk antibody (IgY) to the recombinant rabies virus proteins produced in *Escherichia coli*. Jpn. J. Infect. Dis. 58, 115–118.

Nawtaisong, P., Keith, J., Fraser, T., Balaraman, V., Kolokoltsov, A., Davey, R.A., Higgs, S., Mohammed, A., Rongsriyam, Y., Komalamisra, N., Fraser, M.J., 2009. Effective suppression of Dengue fever virus in mosquito cell cultures using retroviral transduction of hammerhead ribozymes targeting the viral genome. Virol. J. 6, 73.

Nigg, A.J., Walker, P.L., 2009. Overview, prevention, and treatment of rabies. Pharmacotherapy 29, 1182–1195.

Ramm, K., Gehrig, P., Plückthun, A., 1999. Removal of the conserved disulfide bridges from the scFv fragment of an antibody: effects on folding kinetics and aggregation. J. Mol. Biol. 290, 535–546.

Reed, L., Muench, H., 1938. A simple method of estimating fifty percent endpoints. Am. J. Hyg. 27, 493–497.

Schnell, M.J., McGettigan, J.P., Wirblich, C., Papaneri, A., 2010. The cell biology of rabies virus: using stealth to reach the brain. Nat. Rev. Microbiol. 8, 51–61.

Stein, C.A., Hansen, J.B., Lai, J., Wu, S., Voskresenskiy, A., Høg, A., Worm, J., Hedtjärn, M., Souleimanian, N., Miller, P., Soifer, H.S., Castanotto, D., Benimetskaya, L., Ørum, H., Koch, T., 2010. Efficient gene silencing by delivery of locked nucleic acid antisense oligonucleotides, unassisted by transfection reagents. Nucleic Acids Res. 38, e3.

Vascotto, F., Campagna, M., Visintin, M., Cattaneo, A., Burrone, O.R., 2004. Effects of intrabodies specific for rotavirus NSP5 during the virus replicative cycle. J. Gen. Virol. 85, 3285–3290.

Vidy, A., El Bougrini, J., Chelbi-Alix, M.K., Blondel, D., 2007. The nucleocytoplasmic rabies virus P protein counteracts interferon signaling by inhibiting both nuclear accumulation and DNA binding of STAT1. J. Virol. 81, 4255–4263.

Willoughby, R.E., Tieves, K.S., Hoffman, G.M., Ghanayem, N.S., Amlie-Lefond, C.M., Schwabe, M.J., Chusid, M.J., Rupprecht, C.E., 2005. Survival after treatment of rabies with induction of coma. N. Engl. J. Med. 352, 2508–2514.

Wörn, A., Plückthun, A., 2001. Stability engineering of antibody single-chain Fv fragments. J. Mol. Biol. 305, 989–1010.

Yamamoto, M., Hayashi, N., Takehara, T., Ueda, K., Mita, E., Tatsumi, T., Sasaki, Y., Kasahara, A., Hori, M., 1999. Intracellular single-chain antibody against hepatitis B virus core protein inhibits the replication of hepatitis B virus in cultured cells. Hepatology 30, 300–307.